IJAME

Int. J. of Applied Mechanics and Engineering, 2025, vol.30, No.4, pp.52-66
DOI: 10.59441/ijame/210541

DYNAMIC ANALYSIS OF CENTRALLY COMPRESSED INHOMOGENEOUS RODS USING THE INITIAL PARAMETERS METHOD

Hoang Thi Minh Thao and Le Thi Thanh*
Faculty of Applied Sciences, Ho Chi Minh City University of Technology and Education,
Ho Chi Minh City, VIETNAM
E-mail: thanhlt@hcmute.edu.vn

This study investigates the dynamic behavior of centrally compressed elastic rods based on Bernoulli's beam theory, incorporating nonlinear terms through the inclusion of squared section rotation angles. We formulate the stability problem under both dead and follower end loads, deriving the corresponding dimensionless state equations. A closed-form analytical solution is obtained for the fundamental case of free transverse vibrations. Using the initial parameters method, we determine eigenstates and analyze how the first four natural frequencies vary with increasing compressive force. Additionally, the study addresses both static and dynamic bending problems under longitudinal loading, offering insights into the coupled effects of compression and inhomogeneity on rod stability and vibration characteristics.

Key words: compressed-bent rod, transverse vibrations, critical force, initial parameter method, natural frequencies.

1. Introduction

Rods are essential load-bearing elements in modern construction, especially in building frames subjected to vertical and transverse loads. These loads arise from structural weight and interactions with horizontal components like slabs and equipment. The behavior of such elements depends not only on geometry and material but also on the interaction between bending and axial forces. Under high compressive loads, rods may lose stability and buckle, exhibiting bending behavior. Therefore, both static and dynamic effects must be considered in their analysis.

There have been many research works and monographs on the theory of elastic stability.

Demidovich studied the methods of the mathematical theory of motion stability that were applied to problems in the theory of rod stability [1].

In Zubchaninov's work [2], modern concepts of stability beyond the limits of elasticity are examined.

Stephen *et al.* introduced the principles and theories of structural stability in [3]. This classic work, relevant to civil, mechanical, and aerospace engineering, covers the fundamental principles of static and dynamic instabilities.

Batista used the Jacobi test to analyze the stability of planar equilibrium configurations for clamp-clamp and clamp-hinge elastic rods [4].

Whitman and DeSilva [5] developed a linear dynamics theory of elastic rods based on the one-dimensional directed continuum theory. Sufficient conditions for the stability, uniqueness, and instability of rods under the influence of dissipative forces and force couples are presented.

In [6] Varadi provided an exact nonlinear stability analysis for rotating elastic rods based on the methods of Movchan and Lyapunov. The rods are described using Cosserat theory, assuming that their cross-sections experience rigid-body rotations while maintaining perpendicularity to the rod's central axis.

Chamekh *et al.* investigated the numerical stability of equilibrium configurations of elastic rods with unilateral frictionless self-contact [7]. The finite element method was employed, incorporating augmented

* To whom correspondence should be addressed

Lagrangian and penalty approaches to enforce the self-penetration constraint. The numerical solution was obtained using the arc-length continuation method.

Cheng *et al.* [8] studied the stability of helically equilibrated, naturally straight, anisotropic rods with clamped ends based on a differential geometric interpretation. This approach associates each slender elastic rod with a curve on the three-dimensional unit sphere, equipped with a Riemannian metric that accounts for the rod's bending and torsional stiffness.

In Lazarus *et al.* [9] developed a theoretical and numerical framework to analyze bifurcations and stability of slender elastic rods, using geometrically exact 3D kinematics with quaternions for orientation representation. They validated their method by comparing numerical results with precision experiments on a naturally curved, heavy rod under extreme twisting, achieving excellent agreement in predicting 3D buckling instabilities and complex equilibrium configurations.

In two recent studies Thanh *et al.* [10, 11], defined the unstable cases of torsional vibrations and bending vibrations of a thin wing for a profile with two axes of symmetry based on Lyapunov's stability theory and incorporating Vlasov's theory.

Huang *et al.* modified the Discrete Elastic Rods (DER) method from a dynamic to a static framework to analyze bifurcation and stability in slender structures in [12]. By computing eigenvalues of the tangential stiffness matrix at each load step, their approach captures both stable and unstable equilibria, critical points, and solution curves, demonstrating its effectiveness on beams, strips, and gridshells.

In Leanza *et al.* [13] the authors analyzed the stability of multi-loop equilibrium configurations of single-loop elastic rings using conventional stability analysis based on the second variation of system energy. Their study, supported by experimental demonstrations, examined circular and straight multi-loop states, reproduced existing results, and explored the stability of six-sided rings and curved-sided hexagrams that fold into straight configurations.

The development of rod stability theory involves accounting for the nonlinear and inelastic properties of materials [14-17].

Recent developments in structural mechanics and thermoelasticity have significantly advanced the modeling of load-bearing elements under complex loading and thermal conditions. Notably, studies involving generalized thermoelastic interactions in functionally graded and semiconducting materials have provided insights into thermal effects on dynamic responses [18-20]. The vibrational behavior of microbeams and rods under axial motion or dual-temperature theories has also been explored to better understand stability under non-classical conditions [21, 22]. Numerical approaches, such as the finite element method, have been effectively employed to study thermal relaxation, mass diffusion, and wave propagation in anisotropic and porous materials [23-25]. These contributions emphasize the importance of incorporating advanced thermal and mechanical coupling into the analysis of elastic rods, especially when considering dynamic stability and resonance phenomena.

Enhancing methods for analyzing the stability of linearly elastic rods and rod systems remains a significant and ongoing area of research. The formulation of analytical models, especially within the dynamic context, supports the development of efficient algorithms applicable to a wide range of boundary conditions and loading types, including both follower and dead loads. These models not only enable direct analysis of elastic behavior but also serve as foundational tools for addressing inelastic or physically nonlinear problems through approximation. Accordingly, the subject of this study aligns with current research needs and contributes to the broader understanding of the stability of straight elastic rods. The study specifically addresses two main aspects: the development and assessment of static and dynamic analytical models for centrally compressed straight rods with constant cross-sections using the initial parameter method, and the refinement of this method to accommodate rods with discrete changes in stiffness along their length.

2. Static and dynamic problems of centrally compressed rods

2.1. Free transverse vibrations under a time-independent longitudinal force

When formulating the problem, a geometrically nonlinear approach was chosen to describe the dynamic states of a straight rod. The nonlinearity arises from the inclusion of terms proportional to the squares of the rotation angles when varying the deformed state in the Lagrange-d'Alembert equation. In the calculation of

stresses according to Hooke's law, nonlinear components are neglected. The Bernoulli hypotheses are considered valid [26, 27]. Within the framework of these hypotheses, the variational equation takes the following form:

$$\begin{aligned}&\int_0^L\left\{\delta\varepsilon_0 EA\varepsilon_0+\delta\kappa_{xy}EJ_z\kappa_{xy}+\delta\kappa_{xz}EJ_y\kappa_{xz}\right\}dx+\int_0^L\left\{\delta\theta_z EA\varepsilon_0\theta_z+\delta\theta_y EA\varepsilon_0\theta_y\right\}dx+\\&+\int_0^L\left(\delta u\rho A\ddot{u}+\delta v\rho A\ddot{v}+\delta w\rho A\ddot{w}\right)dx-\int_0^L\left(\delta uq_x+\delta vq_y+\delta wq_z+\delta\theta_z m_z+\delta\theta_y m_y\right)dx-\\&+\delta u(0)N(0)-\delta v(0)Q_y(0)-\delta w(0)Q_z(0)-\delta\theta_z(0)M_z(0)-\delta\theta_y(0)M_y(0)-\\&+\delta u(L)N(L)-\delta v(L)Q_y(L)-\delta w(L)Q_z(L)-\delta\theta_z(L)M_z(L)-\delta\theta_y(L)M_y(L)=0,\end{aligned}\tag{2.1}$$

$$\varepsilon_0(x)=\frac{\partial u(x)}{\partial x},\quad \kappa_{xy}(x)=\frac{\dfrac{\partial^2 v(x)}{\partial x^2}}{\sqrt{1-\theta_z^2}},\quad \kappa_{xz}(x)=\frac{\dfrac{\partial^2 w(x)}{\partial x^2}}{\sqrt{1-\theta_y^2}}.$$

Let the longitudinal force be known and time-independent; then, the characteristics of the bending state are determined:

$$\begin{aligned}&\int_0^L\left\{\delta\kappa EJ\kappa-\delta v\rho A\ddot{v}+\delta\theta\cdot N\cdot\theta-\delta vq_y-\delta\theta\cdot m\right\}dx+\\&-\delta v(0)Q(0)-\delta\theta(0)M(0)-\delta v(L)Q(L)-\delta\theta(L)M(L)=0.\end{aligned}\tag{2.2}$$

Differential equation for planar dynamic bending considering the effect of longitudinal force [28, 29]:

$$EJv^{IV}+\rho A\ddot{v}-\left[N'(x,t)\theta+N(x,t)\theta'\right]=q_y.\tag{2.3}$$

It should be noted that the eigenfunctions must satisfy homogeneous boundary conditions, which depend on the fixation of the rod:

- Force boundary conditions: the coefficient at $\delta u(0)$ or $\delta u(L)$ is zero if the displacement at one of the ends is not specified ($\delta u(0)\neq 0$ or $\delta u(L)\neq 0$):

$$\begin{aligned}&EJv''(L)-M(L)=0,\quad EJv''(0)+M(0)=0,\\&-EJv'''(L)+N(L)\theta(L)-Q(L)=0,\\&EJv'''(0)-N(0)\theta(0)-Q(0)=0.\end{aligned}\tag{2.4}$$

- Kinematic boundary conditions:

$$v(0)=v_0,\quad \theta(0)=\theta_0,\quad v(L)=v_k,\quad \theta(L)=\theta_k.\tag{2.5}$$

Note that the terms $N(L)\theta(L)$ and $N(0)\theta(0)$ in the force boundary conditions, representing the projection of the longitudinal force acting on the ends onto the normal to the deformed axis, should be considered only in the case of a 'dead' longitudinal load; for a follower load, these projections are absent.
The system of bending equations for a given longitudinal force can be written in matrix form:

$$y_B^{'} = \mathrm{A}(x,t)_B\, y_B - \mathrm{M}_B \ddot{y}_B + q_B, \quad y_B = \{v \quad \theta \quad M \quad Q\},$$

$$\mathrm{A}(x,t)_B = \begin{bmatrix} 0 & 1 & 0 & 0 \\ 0 & 0 & -\dfrac{1}{EJ} & 0 \\ 0 & 0 & 0 & 1 \\ 0 & N'(x) & \dfrac{N(x)}{EJ} & 0 \end{bmatrix}, \quad \mathrm{M}_B = \begin{bmatrix} 0 & 0 & 0 & 0 \\ 0 & 0 & 0 & 0 \\ 0 & 0 & 0 & 0 \\ \rho A & 0 & 0 & 0 \end{bmatrix}, \tag{2.6}$$

$$q_B = \{0 \quad 0 \quad 0 \quad q_y(x,t)\}$$

where y_B is the state vector for bending, A_B is the model matrix, M_B is the inertia matrix, and $\boldsymbol{q}_B$ is the distributed load vector.

Let us express the system of state equations in a dimensionless form using the relative coordinate $\xi = x / L$ and the following dimensionless variables: $\varpi = v / L$, θ, $\mu = ML / EJ$, $\Theta = QL^2 / EJ$, $n^2 = NL^2 / EJ$, $\gamma_x = q_x L / EA$, $\gamma_y = q_y L^2 / EJ$, $\Omega^4 = \omega^2 T^2 = \rho A L^4 / EJ$, $T_x = \rho L^2 / ET_y^2 = \rho A L^4 / EJ$, $r^2 = \left(T_x / T_y\right)^2 = J / AL^2$ as the dimensionless radius of gyration of the cross-section and the dimensionless time $\tau = t / T$. Then, the state Eqs (2.5) are simplified to:

$$\psi'(\xi,\tau) = A\psi(\xi,\tau) - M\ddot{\psi}(\xi,\tau) + \gamma(\xi), \quad \psi(\xi,\tau) = \{\varpi \quad \theta \quad \mu \quad \Theta\},$$

$$\psi = \begin{bmatrix} 0 & 1 & 0 & 0 \\ 0 & 0 & 1 & 0 \\ 0 & 0 & 0 & 1 \\ 0 & \dfrac{\partial}{\partial\zeta}\left[n^2(\xi)\right] & n^2(\xi) & 0 \end{bmatrix}, \quad M = \begin{bmatrix} 0 & 0 & 0 & 0 \\ 0 & 0 & 0 & 0 \\ 0 & 0 & 0 & 0 \\ 1 & 0 & 0 & 0 \end{bmatrix}, \tag{2.7}$$

$$\gamma = \{0 \quad 0 \quad 0 \quad \gamma_y(\xi,\tau)\}$$

The main problem is determining the system of eigenfunctions of Eq.(2.7). Note that the eigenfunctions must satisfy the homogeneous boundary conditions (2.2), (2.3), and (2.4), (2.5). Since Eq.(2.7) is an ordinary differential equation, the Cauchy problem (initial value problem) can be easily solved for it:

$$\boldsymbol{Y}(x,\omega) = \mathrm{V}(x,\omega)\boldsymbol{Y}(0,\omega) = \mathrm{V}(x,\omega)\boldsymbol{Y}_0(\omega). \tag{2.8}$$

Here, $\mathrm{V}(x,\omega)$ is the normalized fundamental solution matrix of Eq.(2.7), possessing the obvious property: $\mathrm{V}(0,\omega) = \mathrm{I}$, where I is the identity matrix. It is convenient to refer to the fundamental solution matrix as the

initial parameter influence matrix or simply the influence matrix. The vector $Y_0(\omega)$, which represents the state amplitudes at the beginning of the rod at $x = 0$, will be referred to as the initial parameter vector.

Note that, in reality, we are solving a boundary value problem, and only half of the total number of initial parameters are known, as determined by the boundary conditions at $x = 0$. The unknown initial parameters are determined from the conditions at the end of the rod at $x = L$. To do this, we express the solution of Eq.(2.8) at the specified point:

$$\boldsymbol{Y}(L,\omega) = \mathrm{V}(L,\omega)\boldsymbol{Y}_0(\omega) \tag{2.9}$$

The number of unknowns in this system of equations is only half of the total. To obtain the required number of equations, we select the rows corresponding to the specified state components at the end of the rod, as given in (2.4) and (2.5). Since the number of such equations equals the number of unknowns, the system of equations has a square matrix that depends on the parameter ω. This system is homogeneous due to the homogeneity of the boundary conditions. The condition for the existence of a nontrivial solution is that the determinant of the system's coefficient matrix equals zero.

$$\det\left\{\tilde{\mathrm{V}}(L,\omega)\right\} = 0\,. \tag{2.10}$$

Here, $\tilde{\mathrm{V}}(L,\omega)$ is the boundary condition matrix at the end of the rod. Since the fundamental solutions of even the linear vibration problem of a rod are transcendental functions, Eq.(2.10) has a countable set of roots and, consequently, a countable set of nontrivial solutions, which correspond to the modes of free vibrations. We shall consider the presence of only real roots in Eq.(2.10) as a criterion for the stability of the initial state. In this case, the eigenmode transverse motions of the rod are harmonic undamped oscillations, and any small kinematic transverse perturbation leads to a deviation from the initial state that does not exceed the order of the perturbation magnitude. This corresponds to a Lyapunov-stable initial state. The appearance of at least one pair of imaginary roots results in the presence of an aperiodic, unboundedly growing component, leading to the instability of the initial state.

To implement this procedure, it is necessary to construct the fundamental solution matrix. Note that for a constant longitudinal force, Eq.(2.7) has an analytical solution for the static case:

$$\mathrm{V}(x,N) = \begin{bmatrix} 1 & x & \dfrac{1}{EJ\alpha^2}\left[\mathrm{ch}(\alpha x) - 1\right] & \dfrac{\mathrm{sh}(\alpha x) - \alpha x}{EJ\alpha^3} \\ 0 & 1 & \dfrac{1}{EJ\alpha}\mathrm{sh}(\alpha x) & \dfrac{1}{EJ\alpha^2}\left[\mathrm{ch}(\alpha x) - 1\right] \\ 0 & 0 & \mathrm{ch}(\alpha x) & \dfrac{1}{\alpha}\mathrm{sh}(\alpha x) \\ 0 & 0 & \alpha\,\mathrm{sh}(\alpha x) & \mathrm{ch}(\alpha x) \end{bmatrix} \tag{2.11}$$

and for the dynamic case:

$$\begin{aligned} V_{1,1} &= \frac{1}{2}\left(1 + \frac{\alpha^2}{\sqrt{4\lambda^4 + \alpha^4}}\right)\cos(p_1 x) + \frac{1}{2}\left(1 - \frac{\alpha^2}{\sqrt{4\lambda^4 + \alpha^4}}\right)\mathrm{ch}(p_2 x), \\ V_{1,2} &= \frac{\sqrt{2}}{2p_2}\left(1 - \frac{\alpha^2}{\sqrt{4\lambda^4 + \alpha^4}}\right)\mathrm{sh}(p_2 x) + \frac{\sqrt{2}}{2p_1}\left(1 - \frac{\alpha^2}{\sqrt{4\lambda^4 + \alpha^4}}\right)\sin(p_1 x), \end{aligned} \tag{2.12}$$

$$V_{1,3}=\frac{1}{EJ\sqrt{4\lambda^4+\alpha^4}}\left[\mathrm{ch}\left(p_2x\right)-\cos\left(p_1x\right)\right],\quad V_{1,4}=\frac{1}{EJ\sqrt{4\lambda^4+\alpha^4}}\left[\frac{\mathrm{sh}\left(p_2x\right)}{p_2}-\frac{\sin\left(p_1x\right)}{p_1}\right],$$

$$V_{2,1}=(EJ)^2\lambda^4V_{1,4},\quad V_{2,2}=V_{1,1},\quad V_{2,3}=\frac{1}{EJ\sqrt{4\lambda^4+\alpha^4}}\left[p_2\mathrm{sh}\left(p_2x\right)-p_1\sin\left(p_1x\right)\right],$$

$$V_{2,4}=V_{1,3},\quad V_{3,1}=-(EJ)^2\lambda^4V_{1,3},\quad V_{3,2}=-(EJ)^2\lambda^4V_{1,3},$$

$$V_{3,3}=\frac{1}{2}\left(1+\frac{\alpha^2}{\sqrt{4\lambda^4+\alpha^4}}\right)\mathrm{ch}\left(p_1x\right)-\frac{1}{2}\left(\frac{\alpha^2}{\sqrt{4\lambda^4+\alpha^4}}-1\right)\cos\left(p_1x\right),\qquad \text{cont. (2.12)}$$

$$V_{3,4}=EJV_{2,3},\qquad V_{4,1}=-(EJ)^2\lambda^4V_{2,4},\quad V_{4,2}=-(EJ)^2\lambda^4V_{1,4},$$

$$V_{4,3}=\frac{\alpha^2-\dfrac{\alpha^4}{\sqrt{4\lambda^4+\alpha^4}}+\dfrac{2\lambda^4}{\sqrt{4\lambda^4+\alpha^4}}}{p_1}\sin\left(p_1x\right)+\frac{\alpha^2+\dfrac{\alpha^4}{\sqrt{4\lambda^4+\alpha^4}}-\dfrac{2\lambda^4}{\sqrt{4\lambda^4+\alpha^4}}}{p_2}\mathrm{sh}\left(p_2x\right),$$

$$V_{4,4}=V_{3,3},\quad p_1=\frac{\sqrt{2}}{2}\sqrt{\sqrt{4\lambda^4+\alpha^4}-\alpha^2},\quad p_2=\frac{\sqrt{2}}{2}\sqrt{\sqrt{4\lambda^4+\alpha^4}+\alpha^2},\quad \lambda^4=\frac{\rho A\omega^2}{EJ},\quad \alpha^2=\frac{N}{EJ}.$$

In static problems, the initial parameter method for a straight homogeneous rod provides well-known critical force values for various support conditions, which coincide with those presented in strength of materials textbooks.

This section presents the results of calculations for the dependence of dimensionless natural frequencies on the dimensionless longitudinal force for different types of rod supports. The results for a cantilever rod are provided here in both conservative and non-conservative formulations.

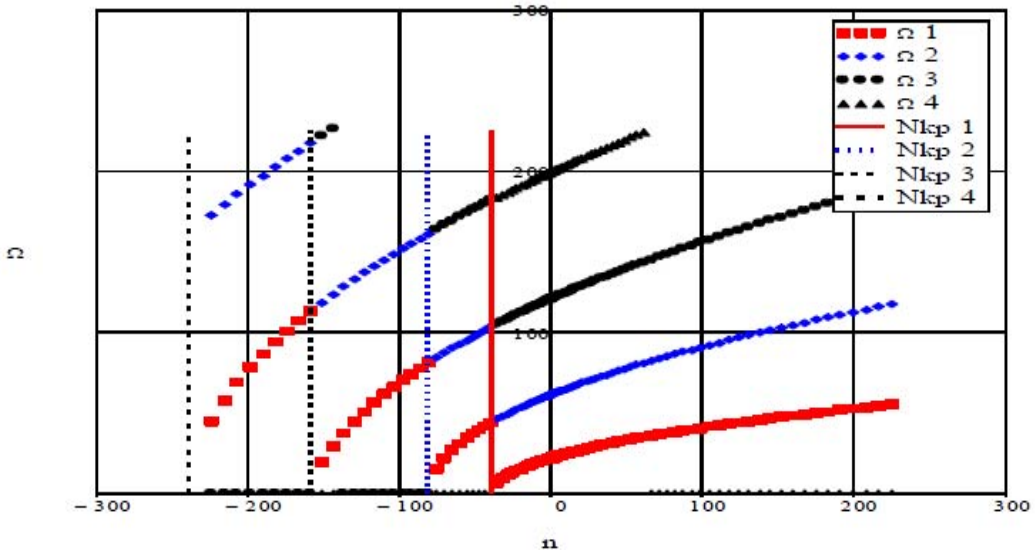

Fig.1. Dependence of the dimensionless natural frequency on the dimensionless longitudinal force for a clamped-free rod ("dead" load).

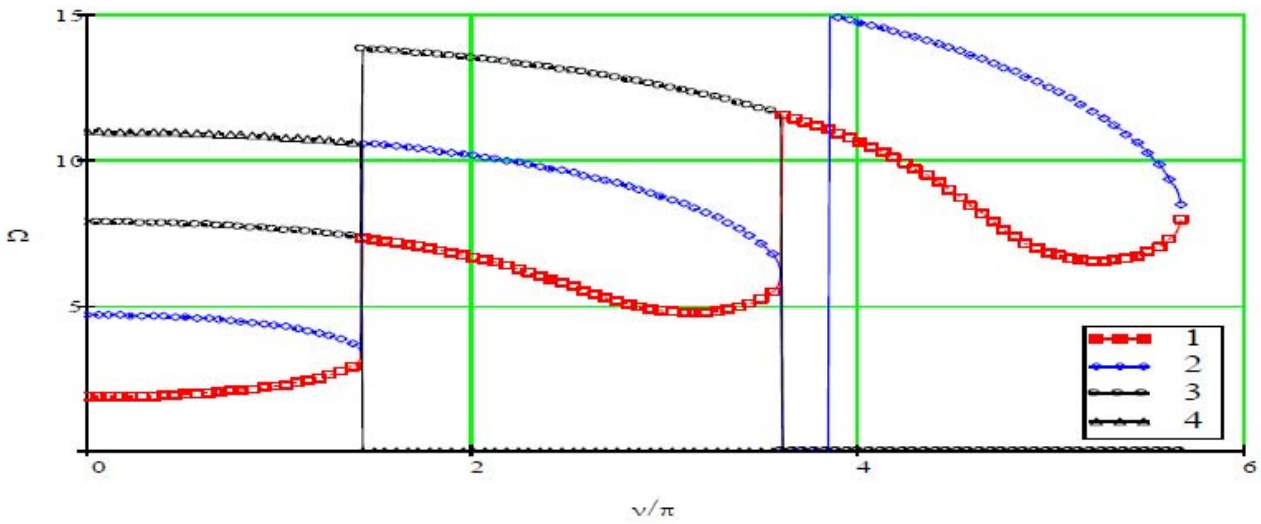

Fig.2. Dependence of the dimensionless natural frequency on the dimensionless longitudinal force for a clamped-free rod (follower load).

In these figures, the vertical lines correspond to the Euler critical force values for different buckling modes. The calculations performed (Figs. 1, 2) show that the Euler critical force, determined in the static formulation, also defines the stability loss point in the dynamic case. The vertical lines corresponding to its value are tangents both to the peaks of the parabolic dependencies $\Omega(n)$ in the conservative formulation (Fig.1) and to the loops of the same dependencies in the non-conservative formulation (Fig.2). At the same time, the nature of bifurcation differs: in the conservative formulation, one mode transitions into an aperiodic motion regime, whereas in the non-conservative formulation, two modes do.

2.2. Free transverse vibrations of a rod under a longitudinal force varying along its length

Consider the case of a distributed longitudinal load that is constant along the length and independent of time. The dimensionless homogeneous equation corresponding to this case has the form:

$$\boldsymbol{\Psi}' = \left(\mathrm{A}^0 + \gamma_x \xi\, \mathrm{S}\right)\boldsymbol{\Psi} + \Omega^2 \mathrm{M}\boldsymbol{\Psi}, \quad \mathrm{A}^0 = \begin{bmatrix} 0 & 1 & 0 & 0 \\ 0 & 0 & 1 & 0 \\ 0 & 0 & 0 & 1 \\ 0 & \gamma_x & n_0^2 & 0 \end{bmatrix}, \quad \mathrm{S} = \begin{bmatrix} 0 & 0 & 0 & 0 \\ 0 & 0 & 0 & 0 \\ 0 & 0 & 0 & 0 \\ 0 & 0 & 1 & 0 \end{bmatrix} \tag{2.13}$$

where Ω is the dimensionless frequency of free vibrations.

To solve Eq.(2.13), we use the method of successive approximations in the form presented in [30], where the initial approximation is taken as the solution of the problem with a constant model matrix

$$\boldsymbol{\Psi}^{0'} = \mathrm{A}^0\boldsymbol{\Psi}^0 + \Omega^2 \mathrm{M}\boldsymbol{\Psi}^0 \tag{2.14}$$

assuming, unlike in [30], that the effect of tension on bending is absent.

Applying the Laplace transform, we obtain the image of the fundamental solution:

$$\boldsymbol{\Psi}^{0^*}(p) = \left\{p\mathrm{I} - \left(\mathrm{A}^0\boldsymbol{\Psi}^0 + \Omega^2 \mathrm{M}\right)\right\}^{-1} \boldsymbol{\Psi}^0(0) = \mathrm{V}(p)^*\boldsymbol{\Psi}^0(0). \tag{2.15}$$

The image of the normalized fundamental solution matrix (influence matrix) has the form:

$$\mathrm{V}^0(p)=\frac{1}{Z(p)}\begin{bmatrix}\left(p^2-n_0^2\right)p-\gamma_x & p^2-n_0^2 & p & 1\\ \Omega^4 & \left(p^2-n_0^2\right)p & p^2 & p\\ \Omega^4 p & \Omega^4+\gamma_x p & p^3 & p^2\\ \Omega^4 p^2 & \left(\Omega^4+\gamma_x p\right)p & \Omega^4+\left(n_0^2 p+\gamma_x\right)p & p^3\end{bmatrix}, \tag{2.16}$$

$$Z(p)=p^4-n_0^2 p^2-\gamma_x p-\Omega^4.$$

The original influence matrix is obtained using the inverse Laplace transform by evaluating the improper integral involved through the residue theorem.

$$\mathrm{V}^0(\xi)=\sum_{k=1}^{3}\frac{e^{\xi p_k}}{Z_1(p_k)}\begin{bmatrix}\left(p_k^2-n_0^2\right)p_k^2-\gamma_x & p_k^2-n_0^2 & p_k & 1\\ \Omega^4 & \left(p_k^2-n_0^2\right)p_k & p_k^2 & p_k\\ \Omega^4 p_k & \Omega^4+\gamma_x p_k & p_k^3 & p_k^2\\ \Omega^4 p_k^2 & (\Omega^4+\gamma_x p_k)p_k & \Omega^4+\left(n_0^2 p_k+\gamma_x\right)p_k & p_k^3\end{bmatrix}, \tag{2.17}$$

$$Z_1(p)=\frac{dZ}{dp}=4p^4-2n_0^2 p-\gamma_x.$$

Let us determine the successive approximations for the solution of Eq.(2.13) as described in [30]:

$$\boldsymbol{\Psi^m}(\xi)=\left\{\mathrm{V}^0(\xi)+\sum_{m=1}^{M}\Delta^m\ \mathrm{V}(\xi)\right\}\boldsymbol{\Psi}(0),$$

$$\Delta^m\ \mathrm{V}(\xi)=\gamma_x\int_0^{\xi}\mathrm{V}^0(\xi-\xi_1)\mathrm{S}\Delta^{m-1}\ \mathrm{V}(\xi_1)\xi_1 d\xi_1. \tag{2.18}$$

Since the upper limit of the integral in (2.18) is finite $(\xi\le 1)$, and from (2.17) it follows that the influence matrix is integrable in the sense of the finiteness of any of its norms, the sequence of increments in (2.18) forms a geometric progression with the first term given by:

$$\Delta^1\ \mathrm{V}(\xi)=\gamma_x\int_0^{\xi}\mathrm{V}^0(\xi-\xi_1)\mathrm{S}\mathrm{V}^0(\xi_1)\xi_1 d\xi_1 \tag{2.19}$$

and the denominator is γ_x, and therefore, it converges in norm for $\gamma_x<1$.

We estimate the magnitude of the dimensionless longitudinal load γ_x. From the expression for the dimensionless load $\gamma_x=q_x L/EA$ we obtain

$$\gamma_x = n_x \frac{g\rho AL^3}{EJ} = n_x \frac{1}{r^2}\frac{g\rho L}{E} = \frac{n_x}{r^2}\frac{L}{L_{mat}}. \tag{2.20}$$

The complex $L_{mat} = E / g\rho$ has the dimension of length and can be referred to as the characteristic size of the material. For real materials (steel, aluminum alloy, fiberglass), this parameter has a value in the range of $(1\ldots3)\ 10^6$ m. The value $r^2 = J / AL^2$ – the dimensionless radius of gyration of the cross-section– for thin rods does not exceed the square of the ratio of the characteristic transverse dimension to the length, meaning it is on the order of 10^2 .Then, the magnitude of γ_x can be estimated as $\gamma_x \sim n_x \cdot 10^{-3}$. The actual values of longitudinal overload are limited to approximately *100*, so γ_x is less than *1*, and successive approximations converge. The following are graphs of norm variations for different numbers of approximations, depending on the longitudinal load at various values of the dimensionless longitudinal load and dimensionless frequency.

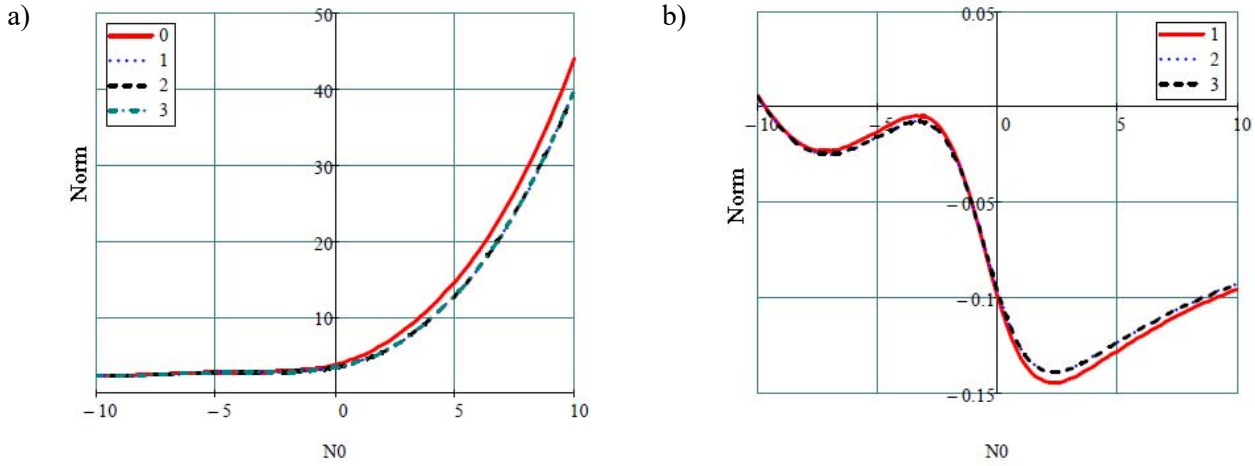

Fig.3. Dependence of the influence matrix norms on the longitudinal force (a) and relative increments (b) for $\gamma_x = 1$, $\Omega = 1$: *0* - initial; *1* - first; *2* - second, etc., approximations.

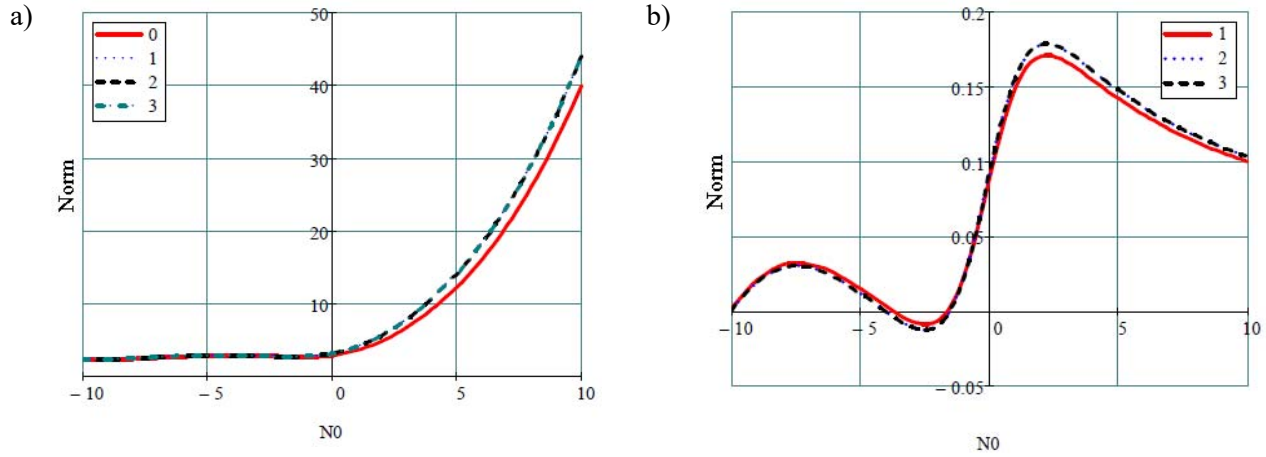

Fig.4. Dependence of the influence matrix norms on the longitudinal force (a) and relative increments (b) for $\gamma_x = -1$, $\Omega = 1$: *0* - initial; *1* - first; *2* - second, etc., approximations.

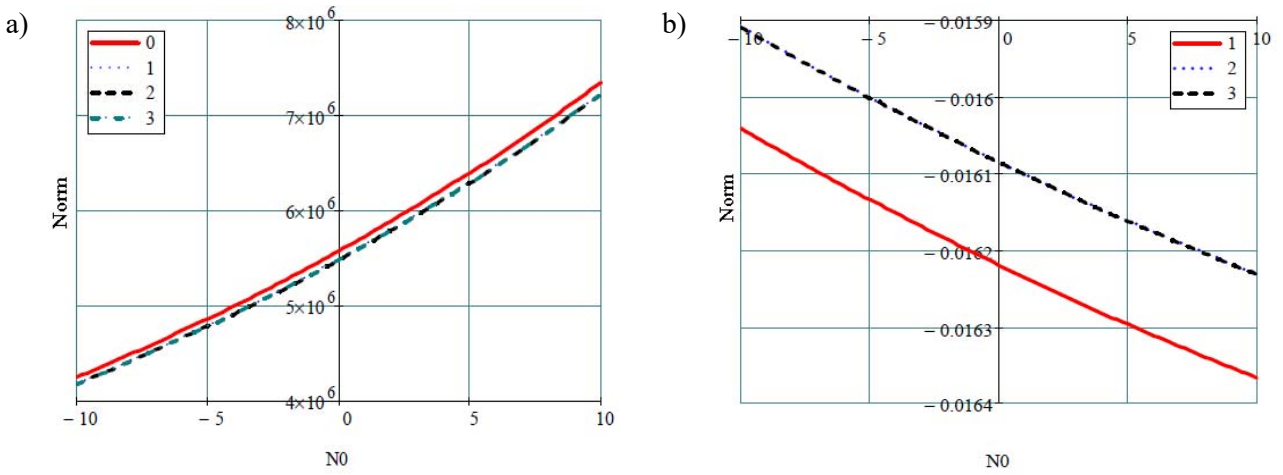

Fig.5. Dependence of the influence matrix norms on the longitudinal force (a) and relative increments (b) for $\gamma_x = 1$, $\Omega = 10$: *0* - initial; *1* - first; *2* - second, etc., approximations.

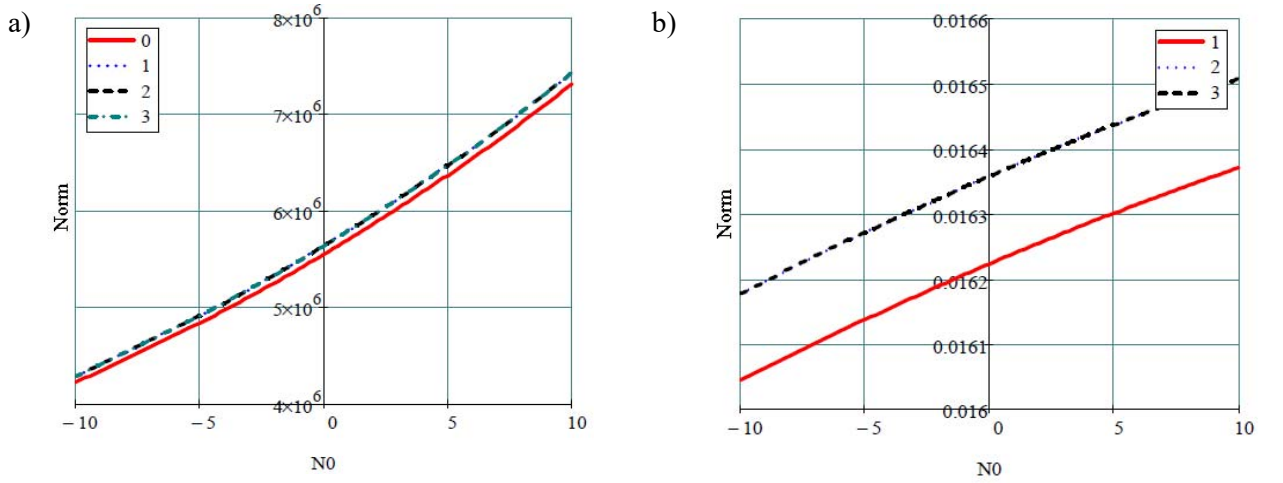

Fig.6. Dependence of the influence matrix norms on the longitudinal force (a) and relative increments (b) for $\gamma_x = -1$, $\Omega = 10$: *0* - initial; *1* - first; *2* - second, etc., approximations.

From Figs 3-6, it is evident that the second approximation contributes the most to the change in the matrix norm, while the third approximation is virtually indistinguishable from the second across the entire range of investigated parameters. At the same time, the parameter γ_x took its extreme values of ± 1. However, convergence was achieved, apparently due to the fact that the integral estimate in Eq.(2.18) is less than *1*. Therefore, for practical calculations, the second approximation is sufficient.

Let us consider the dependence of natural frequencies on the longitudinal compressive load, assuming that its gradient (longitudinal distributed load) takes its extreme values at which convergence is achieved (± 1).

Comparing Figs 7-9 with Fig.1, it is easy to notice that they differ only in the direction of the n^2 axis, and it would seem that the effect of the distributed load is negligible. However, if we plot the graph of the relative deviation of the first frequency without considering the distributed load and with it taken into account (Fig.10), it is easy to observe that near the critical values (π^2, $4\pi^2$, $9\pi^2$, etc.), deviation spikes occur, reaching up to *75%* of the nominal frequency calculated at $\gamma_x = 0$ in absolute magnitude.

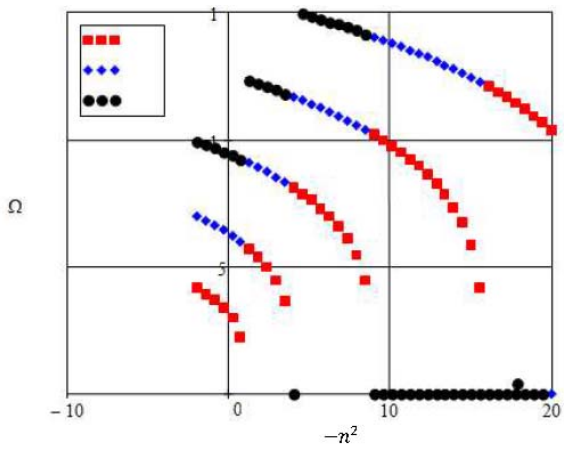

Fig.7. Dependence of the natural vibration frequencies Ω on the dimensionless longitudinal force at $\gamma_x = 0$.

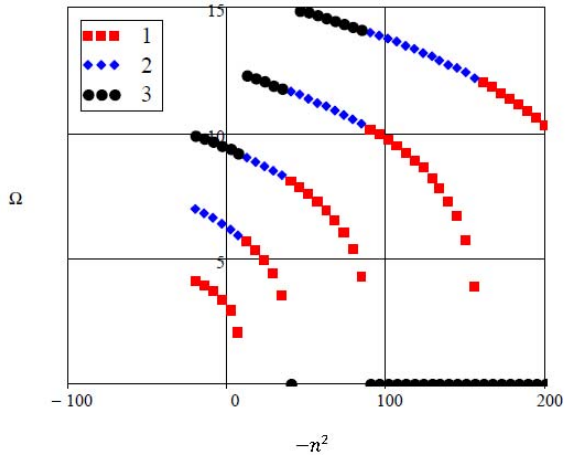

Fig.8. Dependence of the natural vibration frequencies Ω on the dimensionless longitudinal force at $\gamma_x = 1$ (compressive load).

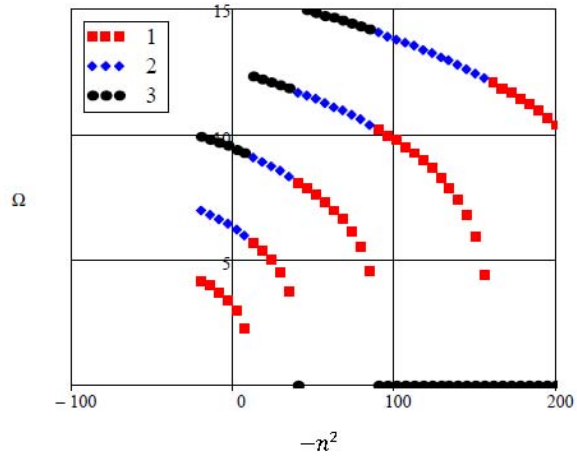

Fig.9. Dependence of natural vibration frequencies Ω on the dimensionless longitudinal force at $\gamma_x = -1$ (tensile distributed load).

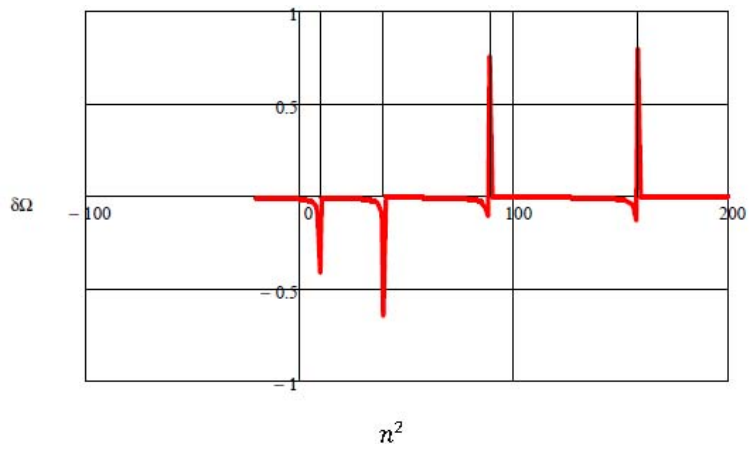

Fig.10. Dependence of the relative deviation of the first natural frequency $\delta\Omega$ at $\gamma_x = 1$ on the frequency at $\gamma_x = 0$.

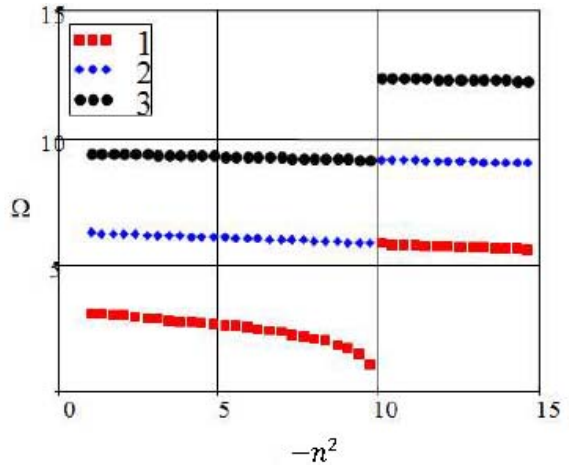

Fig.11. Dependence of the natural frequencies Ω on the dimensionless axial force at $\gamma_x = 0$ near the first critical force.

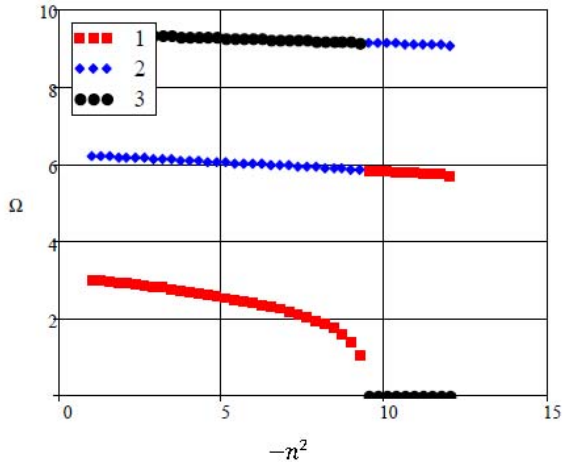

Fig.12. Dependence of natural vibration frequencies Ω on the dimensionless longitudinal force at $\gamma_x = 1$ (compressive load) near the first critical force.

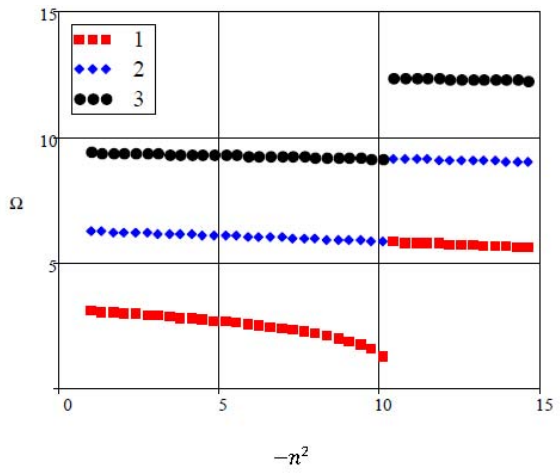

Fig.13. Dependence of natural vibration frequencies Ω on the dimensionless longitudinal force at $\gamma_x = -1$ (tensile load) near the first critical force.

To investigate the effect of the distributed load, the dependencies $\Omega\left(n^2\right)$ were plotted in the range of axial compressive loads close to the first critical force π^2 (Figs 11-13). Comparing these figures, we can observe that the vertical tangent at the peak of the lower curve shifts to the left under a compressive distributed load (i.e., reducing the critical force) and to the right under a tensile distributed load (i.e., increasing the critical force).

3. Conclusions

The initial parameter method proves to be a versatile and effective tool for analyzing the elastic stability of straight rods in both static and dynamic contexts, encompassing conservative and non-conservative systems. For classical problems such as Euler buckling or compressed struts, closed-form analytical solutions can be obtained. In more complex scenarios, the determination of critical loads reduces to solving transcendental equations, which can be efficiently handled using standard computational tools like MathCad and MATLAB.

A key strength of the method lies in its algorithmic universality, achieved through analytical representations of the fundamental solution matrices and frequency equations under various boundary conditions. In cases involving distributed longitudinal loads, the stability problem transforms into a system of differential equations with coefficients linearly dependent on the longitudinal coordinate. The corresponding fundamental solution matrix is constructed using the method of successive approximations, which has been shown to converge rapidly-typically within two to three iterations in dimensionless form.

The study further demonstrates that distributed longitudinal loads significantly affect stability behavior near bifurcation points. Specifically, tensile distributed loads enhance stability by increasing the critical force, while compressive loads have the opposite effect. The magnitude of this influence is approximately *10%* of the distributed load's value compared to the case without it.

Nomenclature

A – cross-sectional area

E – Young's modulus

J – principal central moment of inertia

L – rod length

M_y, M_z – bending moments at the ends of the rod

m_y, m_z – distributed bending moments along the length

N – longitudinal force

Q_y, Q_z – transverse forces

q_x, q_y, q_z – distributed loads along the length of the rod

t – time

u, v, w – components of the vector of displacement of a point in the principal central coordinate system

x – axis of the rod

y, z – the principal central axes of inertia of the cross-section

δ – kinematically admissible variation

θ – angle of rotation of the section

θ_z, θ_y – angles of rotation of the cross-section relative to the binormal and normal, respectively

ρ – material density

References

[1] Demidovich B.P. (1967): *Lectures on the Mathematical Theory of Stability*.– Nauka, Moscow, p.472.

[2] Zubchaninov V.G. (2005): *Strength of Materials.*– Tver, TSTU, p.305.

[3] Timoshenko S.P. and Gere J.M. (2012): *Theory of Elastic Stability*.– Courier Corporation, Technology & Engineering, p.560.

[4] Batista M. (2015): *On stability of elastic rod planar equilibrium configurations*.– International Journal of Solids and Structures, vol.72, pp.144-152, https://doi.org/10.1016/j.ijsolstr.2015.07.024.

[5] Whitman A.B. and DeSilva C.N. (1972): *Stability in a linear theory of elastic rods*.– Acta Mechanica, vol.15, pp.295-308, https://doi.org/10.1007/BF01304297.

[6] Varadi P.C. (2001): *Conditions for stability of rotating elastic rods*.– Proceedings: Mathematical, Physical and Engineering Sciences, vol.457, pp.1701-1720, http://www.jstor.org/stable/3067225.

[7] Chamekh M., Mani-Aouadi S. and Moakher M. (2014): *Stability of elastic rods with self-contact*.– Computer Methods in Applied Mechanics and Engineering, vol.279, pp.227-246, https://doi.org/10.1016/j.cma.2014.06.027.

[8] Cheng Y.C., Feng S.T. and Hu K. (2016): *Stability of anisotropic*, *naturally straight*, *helical elastic thin rods*.– Mathematics and Mechanics of Solids, vol.22, No.11, pp.2108-2119, https://doi.org/10.1177/1081286516657856.

[9] Lazarus A., Miller J.T. and Reis P.M. (2013): *Continuation of equilibria and stability of slender elastic rods using an asymptotic numerical method*.– Journal of the Mechanics and Physics of Solids, vol.61, No.8, pp.1712-1736, https://doi.org/10.1016/j.jmps.2013.04.002.

[10] Thanh L.T. (2023): *Determination of the critical velocity of a straight wing with a high aspect ratio*.– International Journal of Applied Mechanics and Engineering, vol.28, No.1, pp.105-117*,* https://doi.org/10.59441/ijame-2023-0010.

[11] Thao H.T.M. and Thanh L.T. (2024): *Bending vibrations of a thin wing for a profile with two axes of symmetry*.– International Journal of Applied Mechanics and Engineering, vol.29, No.4, pp.106-120. https://doi.org/10.59441/ijame/194850.

[12] Kobelev V. (2022): *Stability optimization for a simultaneously twisted and compressed rod*.– Multidiscipline Modeling in Materials and Structures, vol.18, No.1, pp.24-42, https://doi.org/10.1108/MMMS-12-2021-0205.

[13] Leanza S., Zhao R.R. and Hutchinson J.W. (2024): *On the elastic stability of folded rings in circular and straight states*.– European J. of Mechanics - A/Solids, vol.104, Supplement, p.105041, https://doi.org/10.1016/j.euromechsol.2023.105041.

[14] Biderman V.L. (1968): *Stability of a rod made of neo-Hookean material*.– Mechanics of Machines and Technologies, No.3, pp.54- 62.

[15] Borisevich A.A. (2001): *Optimization of Nonlinear Elastic Rod Systems by the Method of Local Linearized Regions*.– Publishing House Brest State Technical University, p.104.

[16]Doronin S.V. and Chursina T.A. (2002): *Modeling of nonlinear behavior of load-bearing structures in problems of risk analysis and safety of technical systems*.– Computational Technologies and Mathematical Models in Science, Engineering and Education Conf. Report abstract., Institute of Computational Technologies of the Siberian Branch of the Russian Academy of Sciences, p.65.

[17]Sidorovich E.M. (1999): *Nonlinear Deformation*, *Static and Dynamic Stability of Spatial Rod Systems*.– Minsk, Belarusian State Polytechnical Academy, p.200.

[18]Abbas I.A. (2015): *Generalized thermoelastic interaction in functional graded material with fractional order three-phase lag heat transfer*.– J. Cent. South Univ., vol.22, pp.1606-1613, https://doi.org/10.1007/s11771-015-2677-5.

[19]Abbas I., Saeed T. and Alhothuali M. (2021): *Hyperbolic two-temperature photo-thermal interaction in a semiconductor medium with a cylindrical cavity*.– Silicon, vol.13, pp.1871-1878. https://doi.org/10.1007/s12633-020-00570-7.

[20]Alzahrani F.S., and Abbas I.A. (2020): *Photo-thermal interactions in a semiconducting media with a spherical cavity under hyperbolic two-temperature model*.– Mathematics, vol.8, No.4, p.585, https://doi.org/10.3390/math8040585.

[21]Carrera E., Abouelregal A.E., Abbas I.A. and Zenkour A.M. (2015): *Vibrational analysis for an axially moving microbeam with two temperatures*.– J. of Thermal Stresses, vol.38, No.6, pp.569-590, https://doi.org/10.1080/01495739.2015.1015837.

[22]Abbas I.A. and Othman M.I.A. (2012): *Plane waves in generalized thermo-microstretch elastic solid with thermal relaxation using finite element method*.– Int. J. Thermophys., vol.33, pp.2407-2423, https://doi.org/10.1007/s10765-012-1340-8.

[23]Abbas I.A., Kumar R. and Chawla V. (2012): *Response of thermal source in a transversely isotropic thermoelastic half-space with mass diffusion by using a finite element method*.– Chin. Phys., vol.21, https://doi.org/10.1088/1674-1056/21/8/084601.

[24]Abbas I.A. (2015): *A GN model for thermoelastic interaction in a microscale beam subjected to a moving heat source*.– Acta Mech., vol.226, pp.2527-2536, https://doi.org/10.1007/s00707-015-1340-4.

[25]Abbas I.A. and Youssef H.M. (2015): *Two-Dimensional Fractional Order Generalized Thermoelastic Porous Material*.– Lat. Am. J. Solids Struct., vol.12, pp.1415-1431, https://doi.org/10.1590/1679-78251584.

[26]Gryazev M.V. (2011): *Applied Problems of Mechanics of Deformable Solids*.– Part 1, Statics of Rods, Tula: Tula State University Publishing House, p.112.

[27]Tolokonnikov L.A. (1979): *Mechanics of a Deformable Solid Body*.– Moscow, Higher School, p.580.

[28]Bolotin V.V. (1961): *Non-conservative Problems of the Theory of Elastic Stability*.– Moscow, Physics and Mathematics State Publishing House, p.340.

[29]Volmir A.S. (1957): *Stability of Deformable Systems*.– Nauka, Moscow, p.984.

[30]Vasina M.V. (2011): *Numerical and analytical method for determining the forms of free vibrations of spatially curvilinear inhomogeneous rods*.– Dissertation for the degree of Candidate of Physical and Mathematical Sciences, Tula, p.129.

Received: March 22, 2025
Revised: September 10, 2025